Mechanism of Retraction of the Trailing Edge during Fibroblast Movement

WEN-TIEN CHEN

Department of Biology, Yale University, New Haven, Connecticut 06520. Dr. Chen's present address is the Department of Biology, University of California at San Diego, La Jolla, California 92093.

ABSTRACT Retraction of the taut, trailing portion of a moving chick heart fibroblast in vitro is an abrupt dynamic process. Upon retraction, the fibroblast tail always ruptures, leaving a small amount of itself attached to the substratum by focal contacts. Time-lapse cinemicrography shows that retraction produces a sudden, massive movement of both surface and cytoplasmic material toward a cluster of focal contacts near the main body of the cell. The appearance of folds on the upper cell surface at this time and the absence of endocytotic vesicles are consistent with this forward movement.

Retraction of the trailing edge, either occurring naturally or produced artificially with a microneedle, consists of an initial fast component followed and overlapped by a slow component. Upon artificial detachment in the presence of iodoacetate, dinitrophenol, and sodium fluoride, and at 4°C, the slow component is strongly inhibited and the fast one only slightly inhibited. Moreover, the tail of glycerinated fibroblasts shortens in the presence of ATP only at a slow rate, which is comparable to that of the slow component observed with the intact cell. Structurally, an extended tail of a fibroblast is highly birefringent, most likely because of the bundles of microfilaments oriented parallel to the long axis of the tail seen in TEM. Most of the birefringence is lost during the fast phase and the rest during the slow phase of retraction. Concurrently, the bundles of microfilaments disappear during the fast phase of retraction and are replaced by a microfilament meshwork. All of these results are consistent with the hypothesis that the initial fast component of retraction is a passive elastic recoil, associated with the oriented bundles of microfilaments, and that the slow component of retraction is an active contraction, associated with a meshwork of microfilaments.

Fibroblast-type cells in culture attach to and spread on planar substrata to form a varying number of highly flattened lamellae. The spreading of these lamellae places the cell under tension (36, 40, 54), and causes it to elongate to varying degrees in the direction of movement. Translocation of the whole cell occurs (*a*) when one of these lamellae spreads at a higher rate to become the largest and therefore the leading one (9, 68), and the trailing end withdraws at a low rate (22), and (*b*) when the trailing portion of the cell, the tail, becomes greatly elongated under the resulting tension, detaches, and rapidly retracts (6, 20, 38, 64), and the leading edge surges ahead (22). Locomotor activity during fibroblast movement thus involves intrinsic mechanochemical forces that can both extend and retract the tail.

Spreading of the leading lamellae appears to be the active feature of cell locomotion; however, were it not for retraction of the trailing edge, the cell as a whole would not become displaced. Although considerable attention has been devoted to the spreading of the leading edge (e.g., 2–5, 9, 36–38, 48, 60), retraction of the trailing edge has been largely neglected (63). It has been shown, however, that haptotactic movement of cells up a gradient in adhesiveness of the substratum (18) is caused primarily by the greater tendency of the trailing edge to detach from less adhesive substrata (37) and that increased spreading at the leading edge can be induced by retraction of the trailing edge (22, 27).

A major stumbling block in the analysis of the movement of fibroblasts in culture has been our inability to predict when and where spreading will occur and when retraction of cell margins will take palce. In the course of my studies on retraction of the trailing edge during fibroblast movement, however, I have found that the tail of moving fibroblasts becomes taut and phase dark, as seen with the phase-contrast microscope, minutes before detachment and abrupt retraction of the trailing

THE JOURNAL OF CELL BIOLOGY · VOLUME 90 JULY 1981 187-200

edge. One can therefore predict when and where retraction will occur normally in moving fibroblasts by phase-contrast microscopy. In addition, one can induce retraction artificially, by disrupting the attachment of a tail to the substratum with a microneedle.

With this system of predictable locomotor activity at hand, retraction of the trailing edge of moving fibroblasts could be studied with a combination of techniques concurrently: various kinds of light microscopy, cinemicrography, micromanipulation, drug treatment, and electron microscopy. The purpose of this study has been to characterize the retraction process of moving fibroblasts in culture, paying particular attention to: (*a*) the changes in contacts when cells detach from the substratum, (*b*) whether retraction is caused by active contraction or passive recoil, or both, and (*c*) changes in cell surface organization, i.e., how the plasma membrane and its associated cortical cytoskeleton relate to retraction.

MATERIALS AND METHODS

Cell Culture

Suspensions of embryonic chick heart fibroblasts were derived from the ventricle of 7- to 8-d embryos. The method of cell culture has been described elsewhere (23). The culture medium routinely used was Dulbecco's modified Eagle's medium (DMEM), supplemented with 10% calf serum and 1% antibiotic-antimycotic solution (Grand Island Biological Co., Grand Island, N. Y.).

Materials

Materials used in this research were obtained as follows: glutaraldehyde (PolyScience Corp., Niles, Ill.); osmium tetroxide (Fisher Scientific Co., Pittsburgh, Pa.); 2,4-dinitrophenol (DNP) (Merck Chemical Division, Merck & Inc., Rahway, N. J.); ATP, ADP, sodium fluoride (NaF), and iodoacetic acid (IAA) (Sigma Chemical Co., St. Louis, Mo.).

Light Microscopy, Micromanipulation, and Cinemicrography

The retraction of fibroblasts, after both natural detachment and artificial detachment with a microneedle, was recorded with cinemicrography. The preparation for the filming chamber, optics (phase contrast and Nomarski differential interference), micromanipulation, and cinemicrography have been described elsewhere (22, 23).

For examining spread fibroblasts with polarization microscopy, a Zeiss Universal microscope was used, with a selected Abbe-type pol condenser oiled to the large glass coverslip of a "sandwich" filming chamber and with the following achromatic stain-free objectives: 40/0.85 pol Z and 100/1.25 pol Z oil. For phase-contrast and polarization microscope examination of the same cell, an achromatic aplanatic phase and interference contrast condenser was used. This facilitated shifting between the two optic systems such that polarized and phase-contrast images of the same cell could be obtained within 8 s (determined by time-lapse filming). Filtered tungsten illumination was used for phase-contrast microscopy. For polarization microscopy, HBO 200 mercury arc illumination was filtered with two heat-reflecting filters, a green filter, and a UV filter to protect cells from heat and UV damage. A λ/30 Brace-Köhler compensator (Carl Zeiss, Inc., New York, N. Y.) was used to measure the extinction angle and the bias compensations. Series of pairs of two photomicrographs at two opposite compensator settings (8) were taken to demonstrate birefringence and it was found that the bias settings vary between 2.5 and 3.5° for maximum contrast.

For examining contact behavior of cells on a glass substratum, a Zeiss Universal microscope was modified for interference reflection microscopy according to the design of Curtis (26) and Izzard and Lochner (48). A Zeiss 100/1.25 epiplanachromat pol oil objective was routinely used to examine a cell with this technique. In some instances, a Zeiss 100/1.3 phase planapochromat oil objective was used. This allows one to examine a cell in phase contrast and then shift to interference reflection microscopy within 2 s. Although the latter objective produced a similar interference pattern, image contrast and resolution seemed to be reduced. The maximum illuminating aperture of these optics was measured according to the method of Izzard and Lochner (48) and gave the same value, 1.1017. All of these studies were recorded on 16-mm time-lapse films (film type, SO115, Kodak) at frame intervals of 1 s, and processed commercially.

Single Cell Technique for SEM and TEM

To examine the ultrastructure of the cell with special reference to its locomotor activity, movement of a fibroblast was recorded by time-lapse filming and then the same cell was fixed for SEM and TEM. The methods for fixation and localization of cells for SEM have been reported elsewhere (23).

For thin-section TEM study, cells were first cultured on cover glasses. With the filming chamber completely assembled, a spread fibroblast was chosen for observation and its location was marked by engraving a circle, 0.5 mm in diameter, with a diamond-tipped object marker (E. Leitz, Inc., Rockleigh, N. J.), around it on the opposite surface of the coverslip. Cells were fixed at various times before and after detachment of the trailing edge, by perfusing the chamber cavity with 2% glutaraldehyde in a phosphate buffer with 2% sucrose, at pH 7.3 and 37°C for 10 min. The chamber was then dissembled at room temperature and the coverslip containing the cells was removed and rinsed with buffer. The cells were postfixed with 1% osmium tetroxide in the same buffer for 10 min. After osmication, cells were washed in buffer, treated with 1% tannic acid in buffer for 10 min, washed again, dehydrated through ethanol, and then flat-embedded by laying face down on a layer of Epon ~1 mm thick in an aluminum weighing pan. The polymerized Epon was separated mechanically from the weighing pan, and the cell of interest was relocated under a dissection microscope with the help of the engraved circle on the cover glass. With watchmaker forceps, a circle matching the original circle engraved on the cover glass, was inscribed on the exposed surface of the Epon. The polymerized Epon block containing the cells was then separated from the cover glass by immersion in liquid nitrogen. A second circle, matching the circle on the other side of the Epon, was inscribed around the cell, and an arrow parallel to the direction of cellular movement was also marked. The sheet of Epon containing the cell of interest was then trimmed by hand to within ~0.1 mm of the desired location, and the plane of sectioning through the cell was recorded by tracing the cell outline from the time-lapse film to aid later interpretation of EM images. Thin sections were stained with uranyl acetate and lead citrate and examined with a Philips 300 microscope operated at 60 kV.

Analysis of Rate of Retraction

The rate and path of tail retraction were analyzed using cytoplasmic vesicles, as cytoplasmic markers, and particles adhering to the surface, as surface markers. Figure 4 illustrates a typical example of such an analysis. Upon retraction of the trailing edge, all markers undergo a sudden forward movement collectively toward a stationary or null border in front of the nucleus which lies at the front perinuclear region of the cell (Fig. 4 *A* and *B*). The cytoplasmic markers at the null border remain stationary during the 1-min period of retraction of the tailing edge. The degree of advance of the trailing edge at a given time was taken as its distance from the null border, and the percentage of its initial length was calculated by dividing it by the initial ditance from the null border. For an experimental group, the mean of measurements at a given time after retraction is usually derived from 6 to 20 independent experiments, and the data are plotted on a semi-logarithmic scale. Standard deviations of each data point are within 5% during the rapid phase of retraction (0-8 s after detachment) and within 8% during the slow phase (16–64 s after detachment). The lines drawn through the points were obtained by a linear regression analysis and an effort was made to include as many points as possible so that the coefficient of determination (r^2) for each line would be >0.95. For an experimental group all measurements fit either one or the other of two exponential curves, e.g., measurements from 0 to 8 s fitting the fast component and data from 16 to 64 s, the slow one. Because the fast and slow components overlap during the initial phase of retraction, the rate constant of the fast component is determined by subtracting the slow phase rate (16–64 s after detachment) from the fast phase rate (0–8 s after detachment).

To compare the retraction of the detached trailing edges under various experimental conditions (see below), the slopes shown in Fig. 5, which represent the rate constants with units of s^{-1}, are used. In 18% of cases, the trailing portions of the cell adhere to the substratum at many sites, such that several minor retractions occur after the trailing edge is detached, rather than a single abrupt retraction. The results derived from these samples were complicated and difficult to analyze and are not included in this report.

Temperature Treatments

Unless otherwise stated, all experiments were performed in a 37°C room. For 4°C treatments, cell cultures were brought into a 4°C room immediately before micromanipulation of the cell, and their culture medium was replaced by new medium cooled to 4°C. About 1–5 min later, the first micromanipulation was performed. For each set of 4°C experiments, three separate operations were performed on three separate cells to detach the training edge, and the results of each were observed for 10 min.

Drug Studies

Phosphate-buffered saline (PBS: 0.14 M NaCl, 2.4 mM KCl, 8 mM Na_2HPO_4, 1.6 mM KH_2PO_4, 1 mM $CaCl_2$, and 0.5 mM $MgCl_2$) was used as the working medium for the study of the effects of metabolic inhibitors on retraction. The metabolic inhibitors used were 0.2 mM DNP, 0.2 mM NaF, and 0.2 mM IAA dissolved together in PBS. This dosage completely blocks visible movement of the cells in culture, including spreading activity at the leading edge and saltatory movement of intracellular particles, within 5 min after application of the drugs.

With the micromanipulation chamber completely assembled, cells with elongate tails were chosen and washed three times with the working medium (PBS) during time-lapse filming. For each set of experiments, the first operation, which produced retraction of the tail with a microneedle in the presence of only the working medium, served as a control. The inhibitor solution was then applied while filming, and the tails of other cells were caused to retract.

Glycerinated Fibroblasts

To glycerinate fibroblasts, a glass coverslip with attached fibroblasts was quickly rinsed with cold (4°C) 1:1 glycerol:Ca^{++}-free PBS at pH 6. It was then kept in this same extraction solution at 4°C for 1 wk to 2 mo. Before each experiment, the coverslip was rinsed with Ca^{++}-free PBS and put in a sandwich filming chamber at 37°C. Contraction solution (PBS + 2 mM ATP) at pH 7.4 was perfused into the filming chamber while filming. PBS + 2 mM ADP was also used to serve as control for ATP-required contraction. Carmine particles added to the contraction solution were used to estimate the flow rate of the solution and the time elapsed between the arrival at the cell periphery of the contraction solution and fibroblast contraction.

RESULTS

General Description

When the trailing portion of an embryonic chick heart fibroblast, "the tail," separates from the substratum, it invariably retracts. This is illustrated in prints of frames taken from a time-lapse film (Fig. 1). The main features of this retraction are representative of 86 fibroflasts observed under similar conditions (see also Fig. 1 in reference 22).

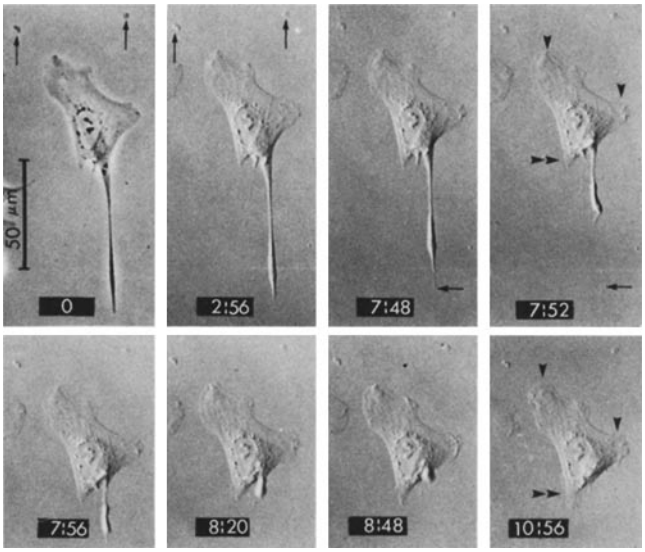

FIGURE 1 Retraction at the trailing edge of an embryonic chick heart fibroblast. Prints of frames were taken from 16-mm time-lapse films. Debris on the substratum serve as fixed reference points (arrows). Numbers on each print refer to minutes and seconds after beginning of the observations. (0) Phase-contrast image of the cell shows a phase-dark tail. (2:56) In this frame and in all subsequent frames the same cell is viewed with Nomarski differential interference optics. Upon detachment, the trailing edge retracts very fast at first (7:48 to 7:56), and then more slowly (7:56 to 8:48). Absorption of the tail remnant into the cell body occurs between 8:48 and 10:56. The retraction is followed by a surge ahead at the two existing spreading edges (arrowheads in 10:56). Note that when it detaches, the trailing edge leaves a part of itself behind (arrows in 7:48 and 7:52). × 300.

Detachment Process

Time-lapse cinemicrography of moving chick heart fibroblasts has revealed that when the trailing edges detach they always leave a part of themselve behind (Fig. 1). This observation is confirmed by SEM (Fig. 2). When such a cell is fixed for examination in SEM, cell surface material is always observed left behind on the substratum in the previous position of the trailing edge (Fig. 2 *C*). Mechanical detachment of the trailing edge with a microneedle also leaves behind ruptured fragments of cell surface on the substratum (Fig. 2 *D*). The ruptured cell surfaces, both the one retained with the cell and the one left on the substratum, appear to seal rapidly, for they appear continuous within 4 s after detachment of the trailing edge (Fig. 2 *D*). Clearly, detachment of the trailing edge of a moving fibroblast from a glass or plastic substratum in culture does not involve separation of the cell surface from the substratum, but rather rupture of the cell surface.[1]

This conclusion is confirmed by observation of the detachment process with interference reflection microscopy (Fig. 3). The trailing edge adheres to the substratum at its tip by means of a cluster of focal contacts (with a spacing ~15 nm between the under surface of the cell and the substratum) and close contacts (with a spacing of ~30 nm) (Fig. 3). As the trailing edge detaches, the contacts remain behind on the substratum. Frame-by-frame analysis of the time-lapse films reveals that these contacts persist for several minutes and then the close contacts fade away, leaving only focal contacts. Upon rupture and retraction, the trailing edge continues to retract until it reaches another cluster of focal contacts near the cell body (Fig. 3). This particular cluster then becomes longer and wider, as the margin continues to retract, and persists until the next detachment. Thus, focal contacts under the tail limit the extent of retraction.

Rate Analysis of Retraction

Time-lapse analysis reveals that retraction of the trailing edge involves a sudden movement of both cell surface (including the plasma membrane and submembranous cortex) and cytoplasm (Fig. 4 *A* and *B*). Fig. 4 *C* shows the results of measurements of the movement of surface and cytoplasmic markers (see Materials and Methods). Measurements on four other cells yielded similar results. Net movement of each marker varies greatly, ranging from 10 to 60 μm, depending on the initial distance of each marker from the null border. In spite of these differences in net movement, however, all measurements of each marker can be fit by two separate exponential curves (Fig. 4 *D*). The slopes of the lines in Fig. 4 *D* fall into two distinguishable ranges. This indicates that the sequence of movement of all markers is similar, e.g., much faster

[1] In view of the finding that "detachment" of the trailing edge from the substratum involves rupture of the cell surface, in a strict sense another term, such as "scission," would be preferable. However, as "detachment" is commonly used for this process, I have decided to continue use of it in this paper, with the understanding that in this case it does not mean that the trailing edge of a fibroblast separates or "deadheres" from the substratum when it pulls away during its locomotion.

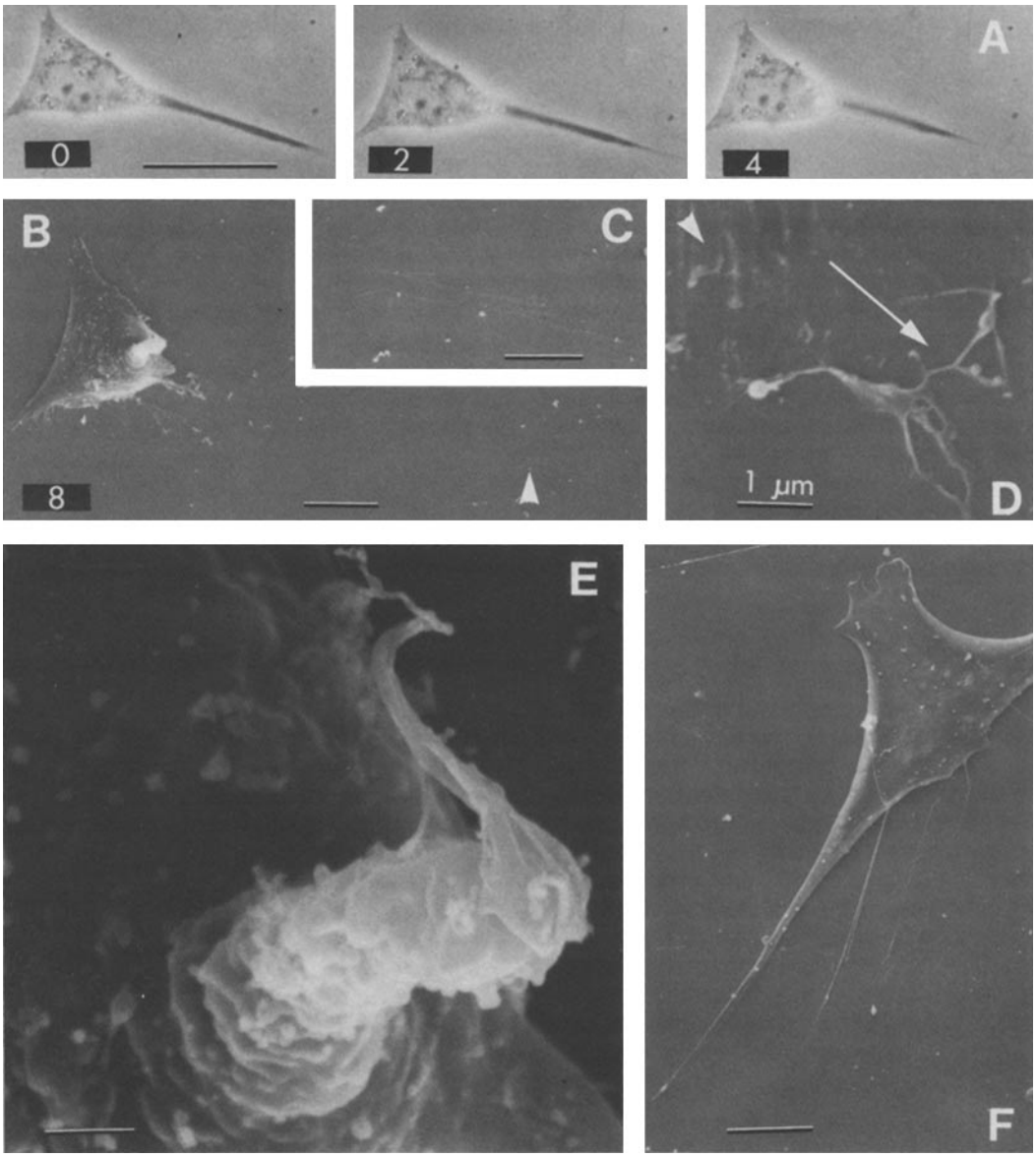

FIGURE 2 SEM micrographs of fibroblasts and their substrata fixed at various times before and after detachment of the trailing edge. (*A*) A fibroblast with a retracting tail in the living state. Numbers on each print refer to seconds after onset of retraction of the trailing edge. Phase-contrast optics. Bar, 30 μm. × 600. (*B*) The cell shown in *A* was fixed at 8 s after onset of retraction of the trailing edge. Note that the tail retracts forward onto the upper side of the cell body, leaving cell surface material behind on the glass substratum (arrowhead). Bar, 10 μm. × 1,000. (*C*) Higher magnification of the ruptured cell surface left behind in the substratum, shown in *B*. Bar, 5 μm. × 2,000. (*D*) Ruptured cell surface remaining on a plastic substratum, fixed 4 s after detachment of the trailing edge of another cell with a microneedle. The arrowhead indicates site of detachment and the arrow points toward the direction of retraction of the tail. Bar, 1 μm. × 10,000. (*E*) Higher magnification of the retracting tail shown in *B*. Bar, 1 μm. × 12,000. (*F*) A spread fibroblast fixed before detachment of the trailing edge. Bar, 10 μm. × 1,100.

at first and slower later, and is independent of their initial position in the cell.

Analysis of the retraction process of a group of cells (Fig. 5) gives results similar to those of the single cell analysis: measurements of tail retraction fit two exponential curves that overlap. The rate constant for the fast component is 6.4×10^{-2} s^{-1} (or 100- to 1,000-fold the normal rate of fibroblast translocation), and the rate constant for the slow component is 9.8×10^{-3} s^{-1} (or 10-fold the rate of translocation). Overall, the initial rapid retraction up to 8 s after detachment of the trailing edge (shown in Fig. 5) is primarily caused by the fast component, and to a small extent (~15% of the initial retraction) by the slow one. The later steady retraction is primarily caused by the slow component.

To determine whether the same sequence of retraction steps occurs whenever the trailing edge is detached, regardless of the cause, retraction of the trailing edge was also induced artificially by detaching the tail from the substratum with a microneedle. This always produces the same sequence of retraction that occurs naturally (Fig. 5).

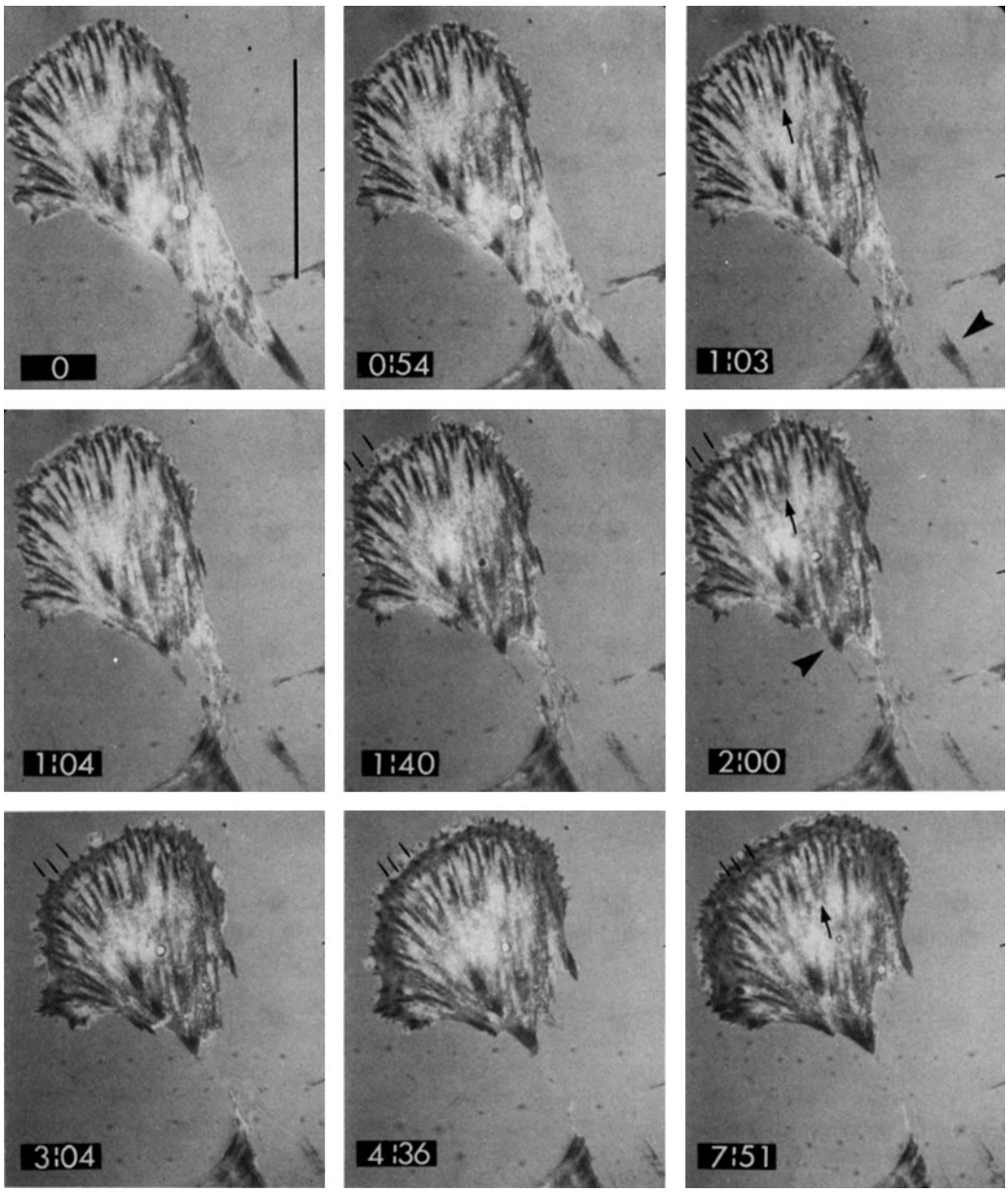

FIGURE 3 Changing pattern of cell-substratum contacts during natural retraction of the trailing edge of an embryonic chick heart fibroblast viewed with interference reflection optics. Numbers on each print refer to minutes and seconds after 1 min before detachment of the trailing edge. This sequence shows the following features. (*a*) Focal contacts, in the form of dark streaks, are located near the broad leading edge and at the tapered trailing end (frame 0). There is also a region of close contact (gray area) just forward of the trailing tip. Elongate dark streaks of focal contacts align parallel to the direction of movement (frame 0 to 1:03). Before detachment of the trailing edge, this pattern of contacts persisted and remained little changed for 15 min. (*b*) The cluster of focal contacts at the trailing edge (arrowhead in frame 1:03) remains behind on the substratum as the trailing edge retracts. Retraction of the trailing edge began at 1:00 (not shown). (*c*) Retraction of the trailing edge stops at the preexisting cluster of focal contacts near the cell body (arrowhead in frame 2:00). (*d*) Increase in protusive activity and, thus, spreading at the leading edge are accompanied by the increase in the uniform gray area of close contacts at the leading edge (2:00 to 7:51). (*e*) New focal contacts form and persist as the new leading edge advances to give rise to the dark streaks seen at the inner margin, while old focal contacts fade. Note formation of three focal contacts indicated by lines in 1:40 to 7:51 and fading of two focal contacts indicated by arrows in 1:03, 2:00, and 7:51. Bar, 50 μm. × 600.

Analysis of the Energy Dependence of Retraction

A number of cellular activities such as lamellipodial extension and withdrawal, ruffling, and saltatory movement of cytoplasmic particles cease within 5 min after fibroblasts are exposed to 4°C, or to media containing metabolic inhibitors, or to glycerination (see Materials and Methods). To examine whether retraction of the trailing edge is also inhibited at the same time as these other aspects of cell movement, the trailing edge was artificially detached by a microneedle under these conditions.

COLD TREATMENT: Detachment of the trailing edge 1–3

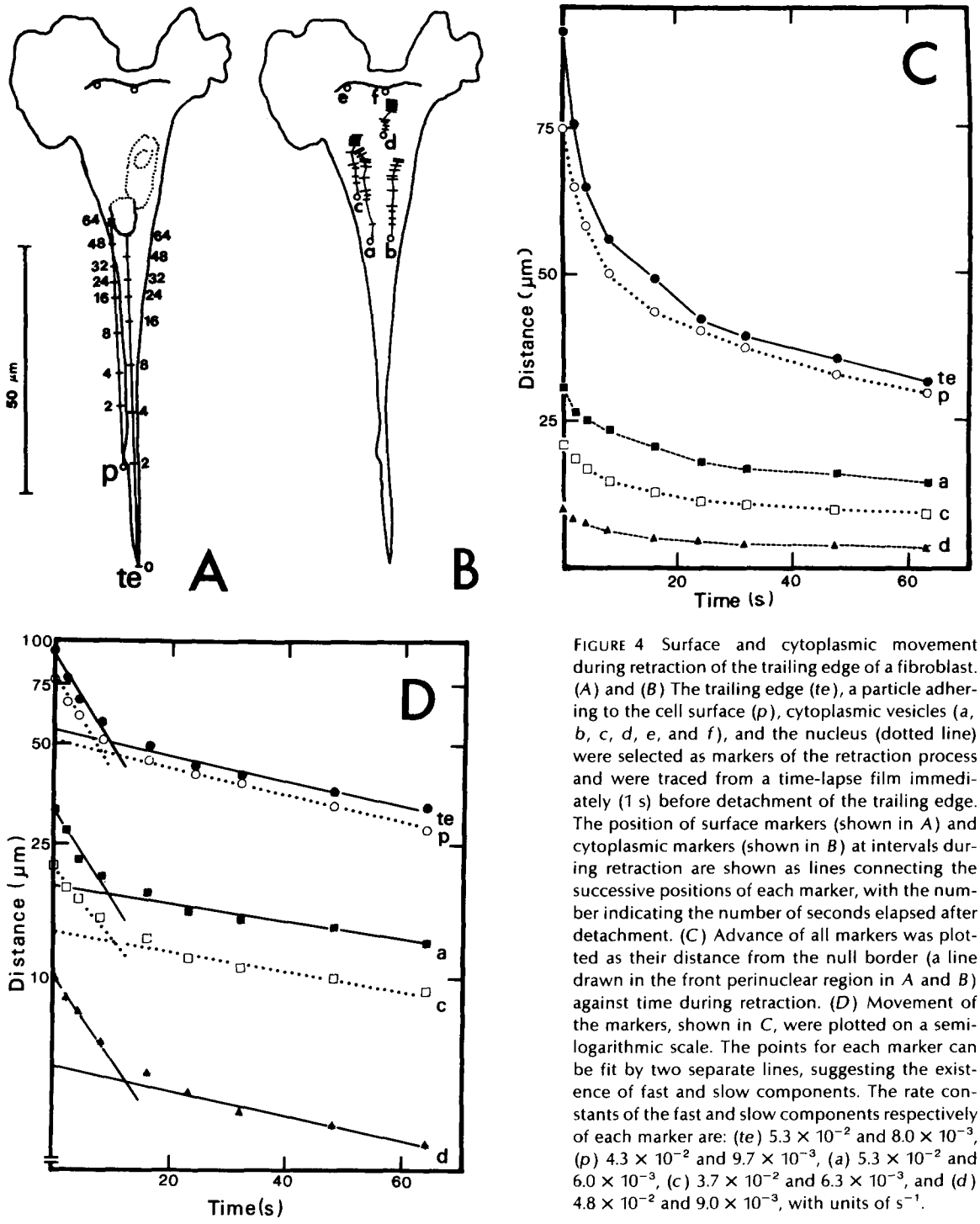

FIGURE 4 Surface and cytoplasmic movement during retraction of the trailing edge of a fibroblast. (*A*) and (*B*) The trailing edge (*te*), a particle adhering to the cell surface (*p*), cytoplasmic vesicles (*a*, *b*, *c*, *d*, *e*, and *f*), and the nucleus (dotted line) were selected as markers of the retraction process and were traced from a time-lapse film immediately (1 s) before detachment of the trailing edge. The position of surface markers (shown in *A*) and cytoplasmic markers (shown in *B*) at intervals during retraction are shown as lines connecting the successive positions of each marker, with the number indicating the number of seconds elapsed after detachment. (*C*) Advance of all markers was plotted as their distance from the null border (a line drawn in the front perinuclear region in *A* and *B*) against time during retraction. (*D*) Movement of the markers, shown in *C*, were plotted on a semilogarithmic scale. The points for each marker can be fit by two separate lines, suggesting the existence of fast and slow components. The rate constants of the fast and slow components respectively of each marker are: (*te*) 5.3×10^{-2} and 8.0×10^{-3}, (*p*) 4.3×10^{-2} and 9.7×10^{-3}, (*a*) 5.3×10^{-2} and 6.0×10^{-3}, (*c*) 3.7×10^{-2} and 6.3×10^{-3}, and (*d*) 4.8×10^{-2} and 9.0×10^{-3}, with units of s^{-1}.

min after exposure to 4°C (Fig. 5) causes an initial retraction. It appears to snap suddenly inward (Fig. 6*A*). The slope for the fast component in the cold is close to that at 37°C; the rate constant of the fast component is 6.8×10^{-2} s^{-1} at 4°C, as compared to 6.5×10^{-2} s^{-1} at 37°C (Fig. 5). However, the fast component of cells exposed to 4°C for more than 10 min is reduced to 50% of the control slope. There is little actual shortening of the tails after this initial rapid retraction (the rate constant of the slow component is 1.7×10^{-3} s^{-1}, as compared to a normal rate of 9.2×10^{-3} s^{-1}). The retracted tail simply slowly twists and waves in the medium (Fig. 6*A*). Thus, the slow component is strongly inhibited.

METABOLIC INHIBITORS: Detachment of the trailing edge with a microneedle in a combination of metabolic inhibitors (see Materials and Methods for time-dosage details) still causes fast retraction, similar to that of cells treated in the cold (Fig. 5). The rate constant for the fast component when treated with metabolic inhibitors is similar to normal. In contrast, the rate constant for the slow component is strongly reduced to 1.6×10^{-3} s^{-1}, as compared to a normal rate of 9.2×10^{-3} s^{-1}. Morphologically, the phase-dark tail becomes phase lucid after the initial rapid retraction (Fig. 6*B*), indicating that its cytoplasmic structure has become disorganized.

GLYCERINATED FIBROBLASTS: Glycerinated fibro-

blasts, with a partially destroyed cell surface (34), do not retract at all in the absence of ATP, even when their trailing edges are detached with a microneedle. The tail of a glycerinated fibroblast, with and without detachment with a microneedle, contracts only after application of PBS supplemented with ATP (Figs. 5 and 6 *C*). This contraction occurs at a slow rate, 0.5 ± 0.1 μm/s (86 measurements), and in a constant manner (Fig. 5). The rate constant for glycerinated fibroblasts, measured as 7.9×10^{-3} s^{-1}, is thus comparable to the slow component of retraction in normal fibroblasts.

Surface Changes during Retraction

Surface changes associated with retraction of the trailing edge were studied by scanning and transmission electron microscopy. Fig. 2 *B* and *E* shows typical SEM micrographs of a cell fixed at the end of the initial rapid phase of retraction of its trailing edge. The upper cell surface of the retracted tail is covered with microfolds, in contrast to that of a spread fibroblast (Fig. 2 *F*), in which the surface is generally and characteristically smooth and free of folds. TEM reveals that the cell surface of the tail becomes folded at the end of the fast phase of retraction (Fig. 10) and that the plasma membrane at the base of some of the folds has amorphous dense material subtending the membrane, resembling coated pits (10, and Figs. 9–11). No pinocytotic vesicles are found under the folded surface of the retracted tail (Fig. 10). These results, along with those with SEM, constitute clear evidence against an internalization of surface membrane by endocytosis, as the trailing edge of the fibroblast retracts.

Changes in Birefringent Pattern upon Retraction

When the trailing edge of a fibroblast is about to detach from the substratum, the whole trailing portion of the cell appears maximally taut and highly refractive, and phase-dark by phase contrast optics (Figs. 1, 6–8). In addition, it is highly birefringent, with birefringent fibrils aligned parallel to its longitudinal axis (Figs. 7 and 8). Upon retraction of the trailing portion of the cell, birefringence typically fades: in most instances this reduction of birefringence occurs first in the front portion of the tail and then at the trailing tip. Time-lapse sequences show that, as a trailing edge of the cell retracts, the tail immediately exhibits a discontinuous pattern of birefringence (Fig. 7), probably indicating helical twisting (see also Fig. 2 *E*). This pattern shortly disappears as the tail slowly retracts, ~8–16 s after detachment of the trailing edge. The cells then become virtually nonbirefringent in the long axis of the retracted tail at the time of maximum retraction and, later, during absorption of the retracted tail into the cell body (Fig. 7).

Changes in Ultrastructure during Retraction

To provide an ultrastructural basis of the changes in birefringence that take place during retraction of the tail of a fibroblast, cells were examined in TEM at various times before and after detachment of the trailing edge. Observations made with light microscopy and electron microscopy correlate well (Figs. 8–10). Bundles of microfilaments are seen to correspond to the phase-dark, birefringent fibrils observed in the tail of a living cell (Fig. 8). Upon retraction, the tails contain only few bundles of microfilaments (Fig. 10 *B*), which corresponds to the reduction of birefringence in the retracting tails. Judging

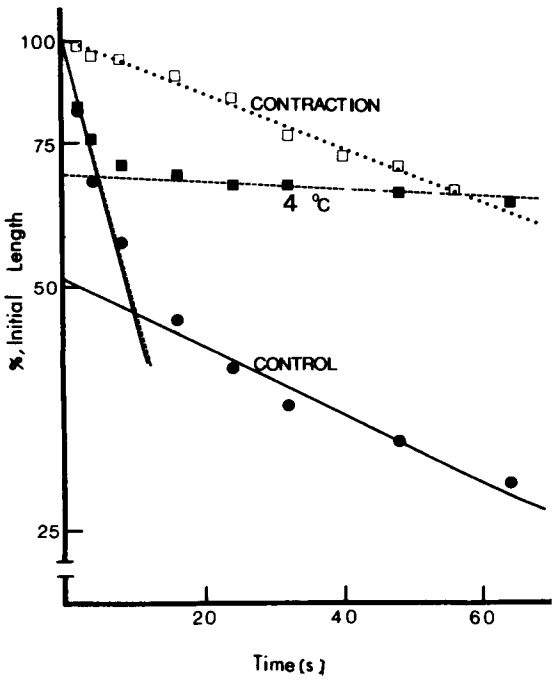

FIGURE 5 Analysis of retraction rates of fibroblasts after detachment of the trailing edge (●) in normal medium at 37°C, (■) at reduced temperature and in the presence of metabolic inhibitors, and (□) after addition of ATP to the glycerinated models.

(●) Data, shown as control, represent the mean degree of retraction of 12 cells following artificial detachment (ADN) of the trailing edge with a microneedle in normal medium at 37°C. Measurements of retraction of another 12 cells after natural detachment (NDN) are not shown in the figure; however, the rate constants of the fast and slow components of both ADN and NDN are listed below. (■) Data designated 4°C are the mean degrees of retraction of six cells, whose trailing edge was detached with a microneedle 1–3 min after the cells were exposed to 4°C medium. These data represent inhibition of the slow component of retraction by cold and metabolic inhibitors. The rate constants of retraction of 12 cells, whose trailing edge were detached between 10 and 30 min after the cells were exposed to 4°C medium (4°C, 10–30 min), and of eight cells, whose trailing edge was detached in the presence of inhibitors (DNP + NaF + IAA), are also given below. (□) Data shown as contraction represent shortening of the detached tails of 12 glycerinated fibroblasts after addition of 2 mM ATP in PBS. Time 0 indicates onset of tail shortening. The rate constant of contraction of glycerinated fibroblasts is 7.9×10^{-3} s^{-1}, whereas the rate constants of the fast and slow components, respectively, of each experiment mentioned above are: (ADN) 6.5×10^{-2} and 9.2×10^{-3}, (NDN) 6.4×10^{-2} and 9.8×10^{-3}, (4°C) 6.8×10^{-2} and 1.7×10^{-3}, (4°C, 10–30 min) 3.5×10^{-2} and 1.0×10^{-3}, (DNP + NaF + IAA) 5.8×10^{-2} and 1.6×10^{-3}, with units of s^{-1}.

from the direction of sectioning and the dispersed images of the microfilaments, I believe that the retracting tails, as shown in Fig. 10, contain mostly meshworks of microfilaments. Furthermore, the microfilament-filled cytoplasmic cortex in the retracting tail becomes enlarged to an average thickness of 0.5 μm (average thickness of cortical microfilaments in a stretched tail is 0.1 μm [see Fig. 9]). From this, it seems likely that bundles of microfilaments present in the elongated tail are reoriented and pulled back into a thickened meshwork upon retraction.

In contrast to microfilaments, the microtubules appear to decrease in number during retraction of the trailing edge. Cross sections along an elongated tail (Fig. 9) contain a constant

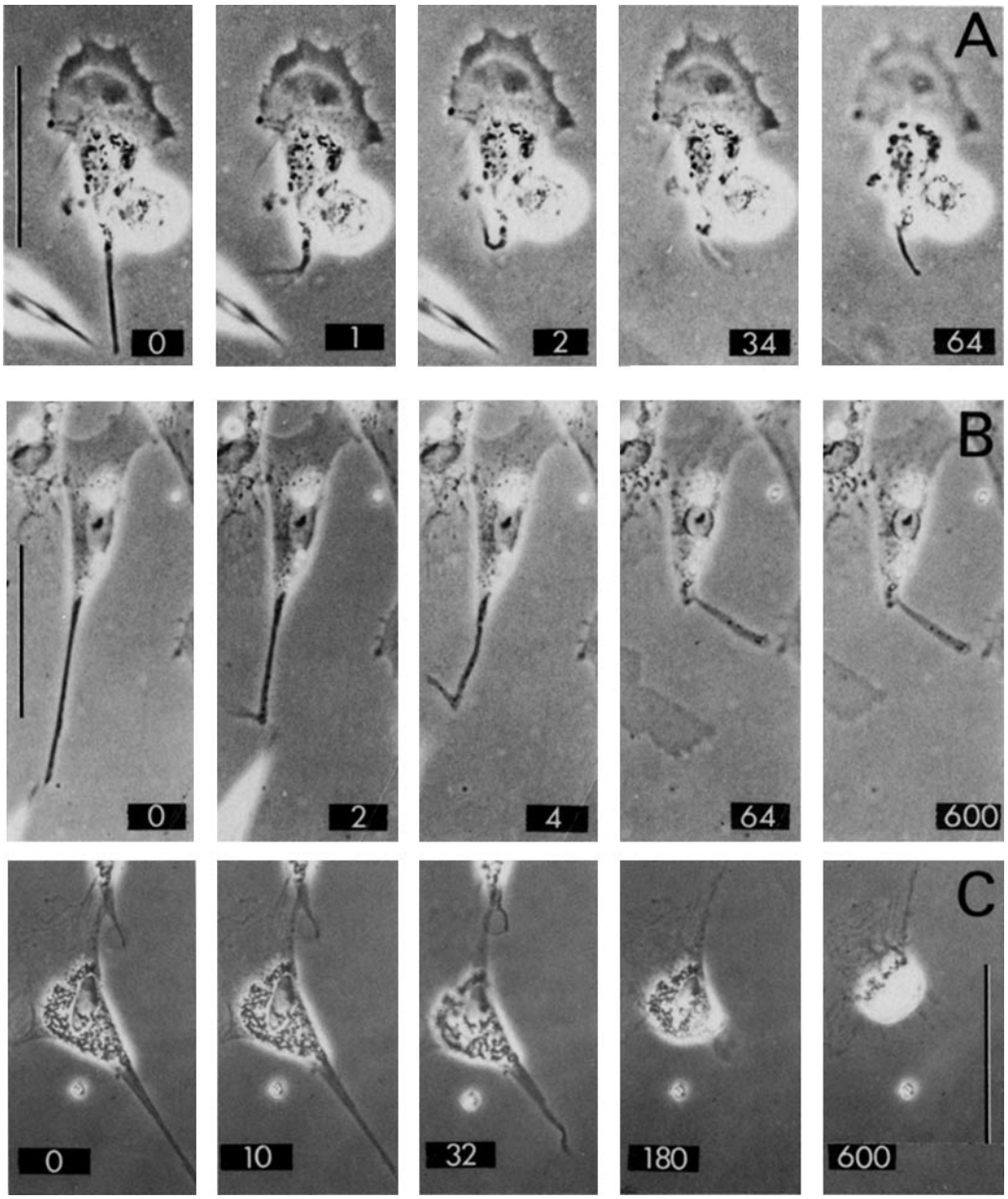

FIGURE 6 Inhibition of retraction of the trailing edge by (*A*) cold, (*B*) metabolic inhibitors, and (*C*) glycerination. Numbers refer to seconds after detachment of the trailing edge with a microneedle. Bars, 50 μm. (*A*) After 20 min at 4°C, the trailing edge snaps forward immediately after its detachment from the substratum, giving the effect of a double exposure in the frame 1 (actual exposure time 0.5 s). Waving, but no actual further shortening, of the tail occurs ~8 s after detachment. × 500. (*B*) Part of the rapid phase of retraction occurs in the presence of 0.2 mM DNP + NaF + IAA in PBS. It also gives a double-exposure image of the tailing edge at frame 2. The retraction soon stops at 8 s after detachment of the trailing edge. × 480. (*C*) Numbers on each print refer to seconds after perfusion with the contraction solution was carried out. Cell surface materials in the broad, thin, leading lamellae were severely extracted by glycerol, while those in the tail seemed to be largely retained, as suggested by the continued phase-dark appearance of the tail at 0 s. the tail starts to shorten (shown in frame 32) ~20 s after addition of the contraction solution. The tail slowly contracts toward the cell body, but the disrupted leading lamellae remain quiescent at 180 and 600 s. × 500.

number of microtubules: 82 ± 6 microtubules (six measurements) are found in the middle portion of the tail and 78 ± 3 (eight measurements) in the region close to the nucleus. During the slow phase of retraction, in two samples examined 16 and 32 s after detachment of the trailing edge, the tails contained less than 10 fragments of microtubules in all sections examined. This nearly tenfold difference in number of microtubules suggests that microtubules are disassembled during retraction. Intermediate filaments become tightly packed and fill the center space of the retracting tails (Fig. 10 *D*), which probably corresponds to the birefringent sphere seen in the retracted cell (Fig. 7).

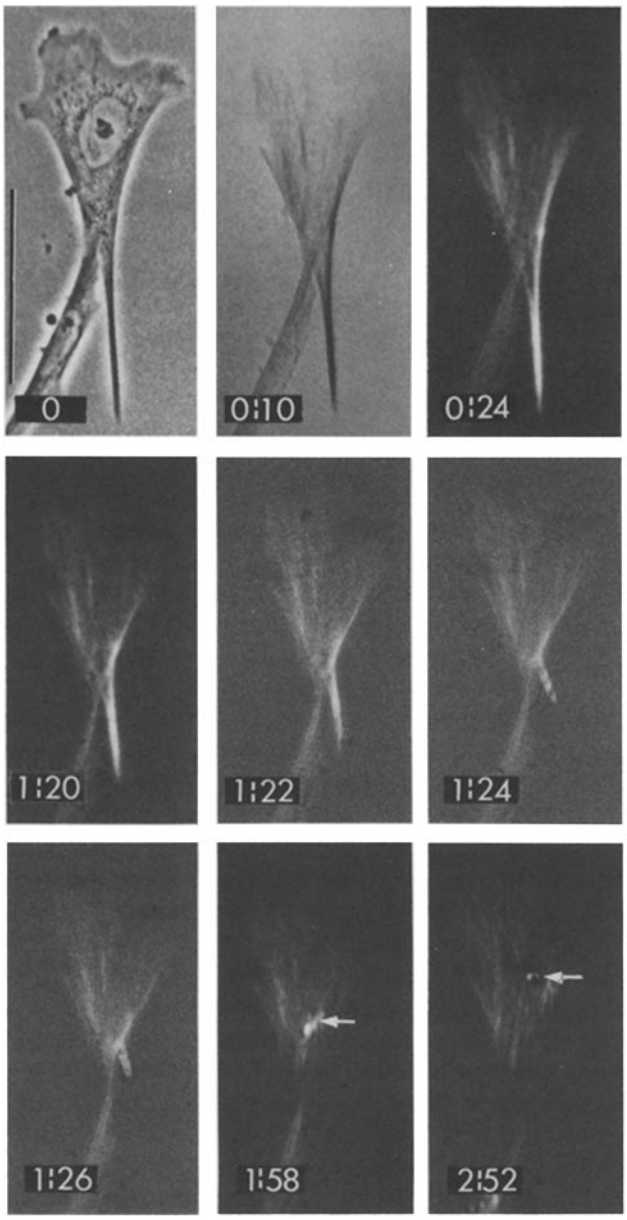

FIGURE 7 Changing patterns of birefringence in a fibroblast during retraction of the trailing edge. Prints of frames were taken from a 16-mm time-lapse film made with phase-contrast and polarization microscopy. Numbers on each print refer to minutes and seconds after beginning of the observations. Phase-contrast image of the spread fibroblast shows the phase-dark tail (frame 0). Reverse contrast of a pair of two prints, shown at 0:10 and 0:24 s, taken at two opposite compensator settings, demonstrates that the fibrils of positive contrast (0:24 to 2:52), parallel to the longitudinal axis of the cell, are indeed caused by birefringence. High contrast prints are presented (0:24, 1:20, 1:58, and 2:52) to show the pattern of birefringent fibrils in the retracting tail and in the cell body. However, three sequential frames after detachment of the trailing edge of the cell (1:22, 1:24, and 1:26) were printed with moderate contrast to show the changing pattern of birefringence in the retracting tail. The retracted tail on the cell body (arrow in frame 1:58) has lost most of its birefringence. A birefringent sphere starts to appear in the cell body at 1:58 and becomes evident at 2:52 (arrows). Note that a trace of birefringent fibrils remains in the cell body after the tail is completely absorbed (frame 2:52). Bar, 50 μm. × 520.

The upper side of the cell body in front of the retracting tail shows the same thickening of microfilament meshwork beneath the folded surface as in the retracting tail itself (Fig. 11 *A* and *B*). In contrast, the upper surface of the cell body behind the retracted tail and, now, the new tail (Fig. 11 *C*) is smooth and contains oriented cortical microfilaments. Concomitantly, the entire underside of the cell body remains generally smooth (Fig. 11). Its cortical microfilaments are aligned in the form of bundles and appear to terminate at the sites of several electron-dense plaques (Fig. 11 *A*, *C*, and *D*). The restriction of folded membrane and associated thickened microfilament meshwork to the retracting tail and adjacent upper cell cortex suggests that contraction of this cortical meshwork is the active force pulling the retracting tail forward during the slow phase of retraction.

DISCUSSION

Rupture of the Trailing Edge upon Retraction

It has been proposed that detachment of cells from other cells or from inert substrate may involve "deadhesion" (24, 26), rupture of cell surface (65), or both. However, it was later demonstrated that when cells are detached artificially from a plane substratum, either by mechanical shearing (65, 67) or by chemical treatment (25), pieces of the cell surface are left behind. Weiss (65, 66) contends that this is usual and normal, and that "distraction" by mechanical shearing provides a measure of strength of the cell surface rather than of the adhesion. The present study clearly demonstrates, by a direct correlation of cinemicrography, SEM and interference reflection microscopy, that nonlethal rupture of the cell surface does indeed occur upon abrupt retraction of the trailing edge of a fibroblast, both during normal cellular locomotion in vitro and after detachment with a microneedle.

Surface Changes during Retraction

In view of the fact that the plasma membrane is fluid at physiological temperatures (58) and that surface constituents move rapidly in fibroblasts (4, 28, 36), the behavior of the upper surface of a fibroblast during tail retraction takes on added interest. Does it flow forward; does it retract elastically; does it fold up into microvilli or other folds (29, 32); or is it internalized in the form of endocytotic vesicles (30)? In this study, analyses of movement of particles on the cell surface and of cytoplasmic vesicles during retraction show that there is a collective movement of the cell surface toward the leading edge of the cell (Fig. 4). Concomitantly, folds and microvillus-like structures appeared on the retracted tail (Fig. 2) and no pinocytotic vesicles were observed beneath the folded surface (Figs. 10 and 11). These results suggest that the cell surface of the retracted tail is temporarily conserved during retraction,

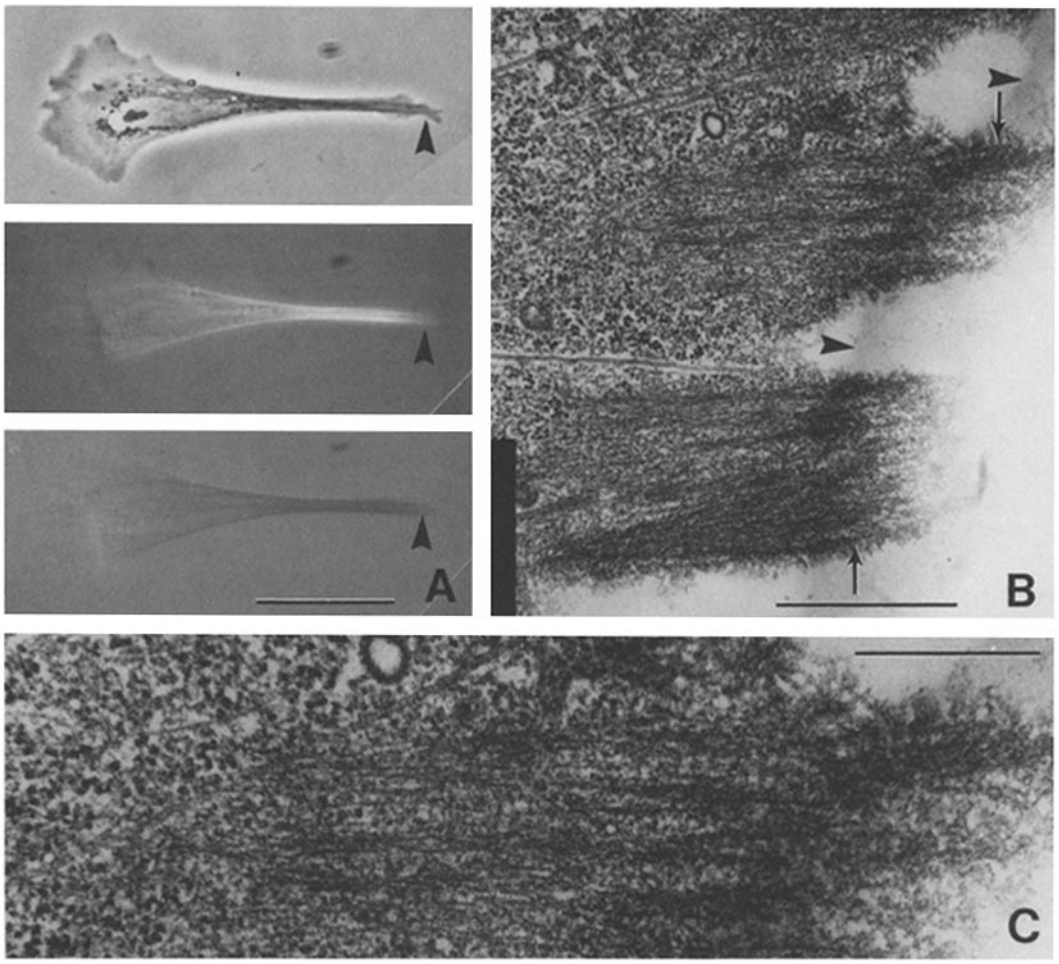

FIGURE 8 A correlation of light microscopy and electron microscopy of the trailing edge of a fibroblast. (*A*) Phase-contrast and polarization microscopy of the same cell. Note the direct correlation of the phase-dark fibrils and birefringent fibrils in the trailing edge of the cell. Bar, 30 μm. × 600. (*B*) Thin section parallel, but with a slight angle, to the plane of cell-substratum contacts throughout the trailing edge of the same cell, shown by arrowheads in *A*. The cell was fixed immediately after the light micrographs were taken. The dark shadow in the right side of the print (arrowheads) is the serum line on the substratum. Because one end of the microfilament bundles (arrows) coexists with the serum line in this section, the end of microfilament bundles in the serum shadow might represent the termination of the bundles of microfilaments on the plasma membrane. Note that the position of the bundles of microfilaments relates to that of phase-contrast and birefringent fibrils. Bar, 1 μm. × 24,000. (*C*) A higher magnification of the section shown in *B*. Note that the individual microfilaments in the bundle are not strictly parallel to one another. Bar, 0.5 μm. × 48,000.

which constitutes clear evidence against an elastic retraction of surface membrane or an internalization of surface membrane by endocytosis. Then, at 15 min after detachment, when the cell is advancing slowly, the upper surface once again becomes smooth (23). This sequence of events suggests that the cell surface that moved forward during tail retraction is soon utilized for the renewed spreading at the leading edge of the cell (22, 27).

Passive and Active Components of Retraction

The shortening of cell processes is generally assumed to involve active contraction (34, 43, 45, 47, 49); however, it could also involve elastic recoil of the cell under tension or a combination of both (63). Although the degree of tension developed by an extended, moving fibroblast has not yet been measured with accuracy (38, 40, 54), it is obviously high (39). The detailed analysis of fibroblast tail retraction in this communication demonstrates that the rate of retraction clearly involves two components: the first with an initial exceedingly fast rate followed and overlapped by a slow one (Figs. 4 and 5). The fast component can be interpreted as elastic recoil, resulting from tension preexisting in the spread cell (35, 44, 62). Shortening of the tail by this means will cease when the declining tension equals the force resisting shortening. After this, the continued steady shortening (the slow phase of retraction) of the tail must be an active contractile process.

Consistent with this conclusion, both metabolic inhibitors and reduced temperature (4°C) strongly inhibit the slow component, leaving the fast component only slightly affected. Furthermore, treating fibroblasts with ionophore A23187 in Ca^{++}-free solution, which presumably lowers free Ca^{++} in the cells and blocks active contraction (47), completely blocks the slow component but has little effect on the fast one (unpublished results). In addition, the tail of glycerinated fibroblasts shortens in the presence of ATP at a slow rate that is comparable to that of the slow conponent of normal retraction. A

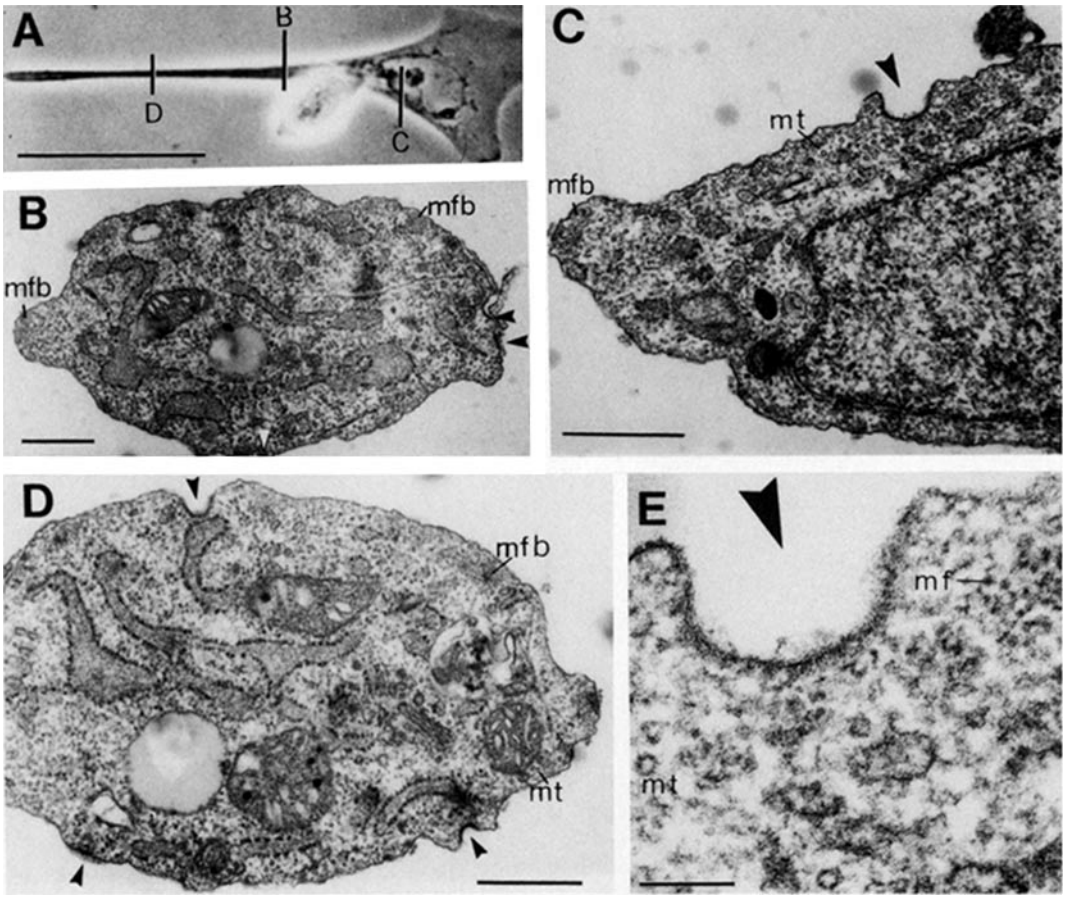

FIGURE 9 Cross sections of an elongate fibroblast. (*A*) Phase-contrast image of the cell in the living state. Bar, 50 μm. × 500. (*B*) A cross section of the tail at the level indicated by a line in *A*. Bar, 0.5 μm. × 18,000. (*C*) A cross section of the cell body indicated by a line in *A*. Bar, 0.5 μm. × 32,000. (*D*) A cross section of the middle portion of the tail indicated by a line in *A*. Bar, 0.5 μm. × 28,000. (*E*) A higher magnification of a portion of cell surface shown in *C*. Bar, 0.1 μm. × 128,000. The aggregates of electron-dense dots in the cortical cytoplasm are cross-sections of bundles of microfilaments (*mfb*). The plasma membrane is not smooth in cross sections. Some regions of the plasma membrane contain amorphous dense material subtending both sides of the membrane (arrowheads). *mt*, Microtubules.

kinetic component of glycerinated fibroblasts comparable to the fast component of normal cells was never seen. This result could be because glycerination disrupts the cell surface and may relax tension in the spread cells. Taking all of these results together, it appears that the fast component represents primarily the passive recoil of a system under tension, whereas the slow component represents an active contraction.

The partial inhibition of the fast component of retraction (Fig. 5) by metabolic inhibitors and cold treatment could be only an apparent one, on account of its overlap with the slow component, or it could be on account of an intrinsic effect on the fast component. If the energy stored in an elastic component results from stretching during spreading, then the development, and possibly the maintenance, of the stretched state may well depend on active processes. Finally, the increased inhibitory effect of prolonged cold treatment could also be due to other effects, such as an increased viscosity of the plasma membrane (19) or depolymerization of cytoplasmic filaments (56).

Structural Basis of Active and Passive Retraction

Since the elongate, taut tail of a moving fibroblast is filled with bundles of microfilaments extending parallel to its long axis (15, 33, 53, 60), the orientation of these filaments before rupture of the trailing edge might provide an ultrastructural basis for the development of tension in the tail. Thin-section electron microscopy has revealed that the individual microfilaments that make up the bundles in the tail are not strictly parallel to one another (Fig. 8). When critical point-dried specimens were examined in whole-mount TEM (15, 16, 21), the oriented microfilaments (bundles) appeared to be oriented regions of the uniquitous filamentous meshwork, somewhat like a three-dimensional fish net under tension (2, 52). This suggests that organization of microfilaments into elongated bundles is produced by tension generated in the cytoplasmic network. If this is so, one prerequisite might be an anchoring of the microfilaments to the plasma membrane. Oriented microfilament bundles terminate at focal sites of cell-substratum contact (5, 14, 41), precisely where tension generation in the cytoplasm would be the strongest and alignment would therefore be the greatest.

If this hypothesis is valid, one would predict that when the trailing edge of fibroblast retracts rapidly, and the tension within the tail is suddenly reduced, the microfilament bundles would lose their orientation and reassume the meshwork arrangement. TEM observations are consistent with this suggestion. Because the domain of cortical microfilaments becomes

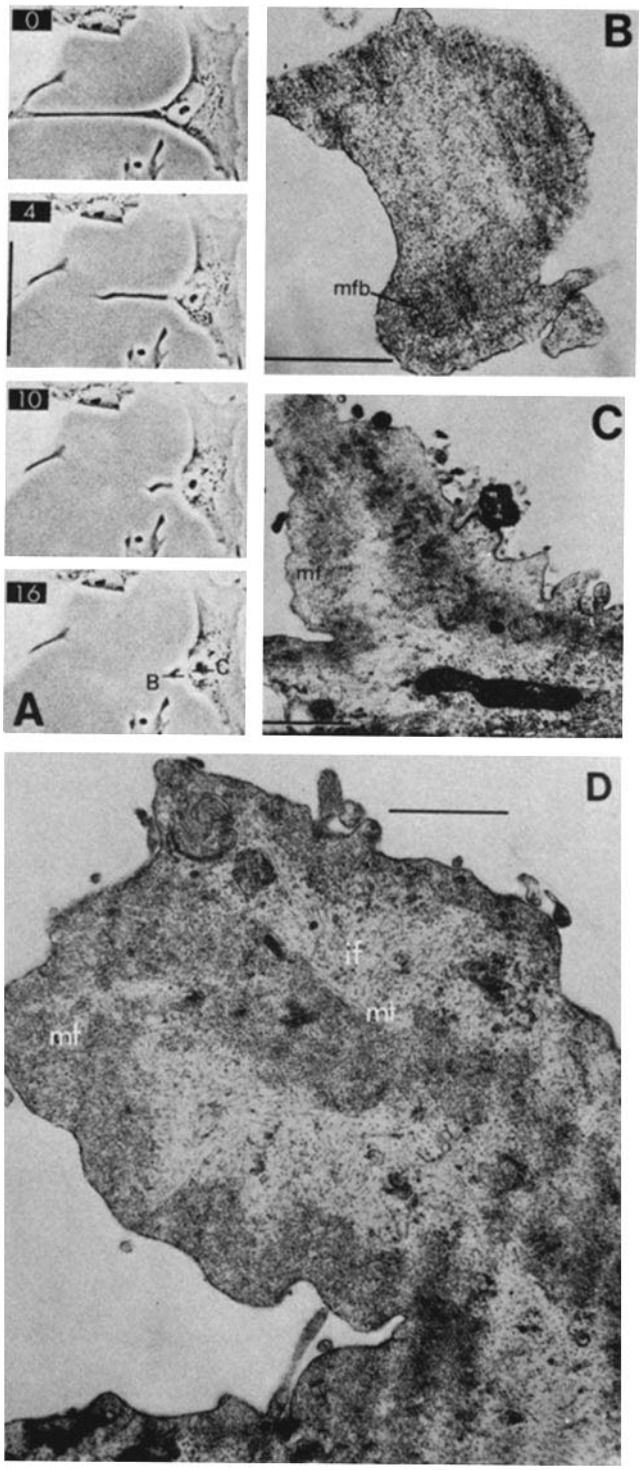

FIGURE 10 Ultrastructure of the retracting tail of a fibroblast. (*A*) Time-lapse sequences of retraction of the trailing edge. The cell was fixed 16 s after detachment of the trailing edge. Bar, 50 μm. × 400. (*B*) A sagittal section of the tip of the retracting tail. Approximate position of the section is shown by the line *B* in *A*. Note the generally random orientation of the microfilaments. A bundle of microfilaments (*mfb*) is identified in the section. Bar, 1 μm. × 15,500. (*C*) A sagittal section of the base of retraction tail close to the cell body. Approximate position of this section is shown by the line *C* in *A*. Note the folded cell surface and the condensed and randomly oriented microfilaments (*mf*). Bar, 1 μm. × 10,400. (*D*) A higher magnification of a sagittal section adjacent to the section shown in *C*. Cortical meshworks of microfilaments (*mf*) are thickened up to 0.75 μm and lie beneath the folded surface. Intermediate filaments (*if*) and a few microtubules (*mt*) are located in the subcortical region. Bar, 1 μm. × 15,500.

thicker when the tail shortens and widens, it seems likely that a reorientation of microfilaments from bundles to meshwork is occurring, rather than a disassembly of the microfilaments themselves. Consistent with this, the highly birefringent extended tail loses much of its birefringence during retraction (Fig. 7). This is also what one would expect if there were a change in the orientation of microfilaments from a longitudinally oriented arrangement parallel to the long axis of the tail to a randomly oriented state. This essential mechanical process, involving no substantial breaking and making of molecular bonds, would fit with the observation that the fast component of tail retraction is not much affected by reduction of temperature or by metabolic inhibitors.

Once this rapid physical reorientation of the microfilaments from bundles to meshwork occurs, the actomyosin meshwork may contract and undergo other chemical rearrangements (11, 13, 17, 45, 47, 50, 57, 61). Such processes might well be markedly inhibited by lowering the temperature and by metabolic inhibitors, and could therefore be the primary events occurring during the slow phase of retraction. The formation of folds in the cell surface during this slow phase would be consistent with the idea that the contraction of the cortical meshwork under the surface provides the active force for tail retraction during this phase.

CONCLUSION

Organization of the Filamentous System in Relation to Tension

The idea that interwoven protein chains in the cell cortex are responsible for the elastic nature of the cell surface was suggested many years ago by Lewis and Lewis (51). They stated that the extending margins of spread cells "produced a pull on the cytoplasmic layer," that "tension striae" were in some way produced by this tension and disappear when the tension is reduced. These tension striae have been identified as a collection of oriented, actin-containing microfilaments (e.g., 12, 34, 46, 59) and referred to variously as "stress fibers" (15), "sheath microfilaments" (60), and more commonly recently as "microfilament bundles" (e.g., 34, 41). In confirmation of this old idea, artificial application of tension to cytoplasmic gels causes the normally randomly oriented filaments to line up parallel to one another (7, 61). Moreover, recent observations have shown that microfilaments in the cortex of *Physarum* become oriented only when contraction is resisted and are, therefore, under increased tension (31, 55). During fibroblast locomotion, plaques and their associated cortical bundles of microfilaments appear within 20 s after cells make contact with other cells (42) and with the substratum (21). This apparently reflects the "contact retraction" (1), which occurs immediately after contact, in which the cell is placed under tension precisely at the sites of close surface apposition.

The present study of retraction of the trailing edge of a moving fibroblast suggests the following mechanism for the process. (*a*) Rupture of the trailing edge causes a loss of tension. (*b*) Loss of tension occurs in two phases, corresponding to an initial fast phase of retraction, followed by a slow one. (*c*) Loss of tension transforms elongated microfilament bundles into a disoriented meshwork in the fast phase. (*d*) Active contraction

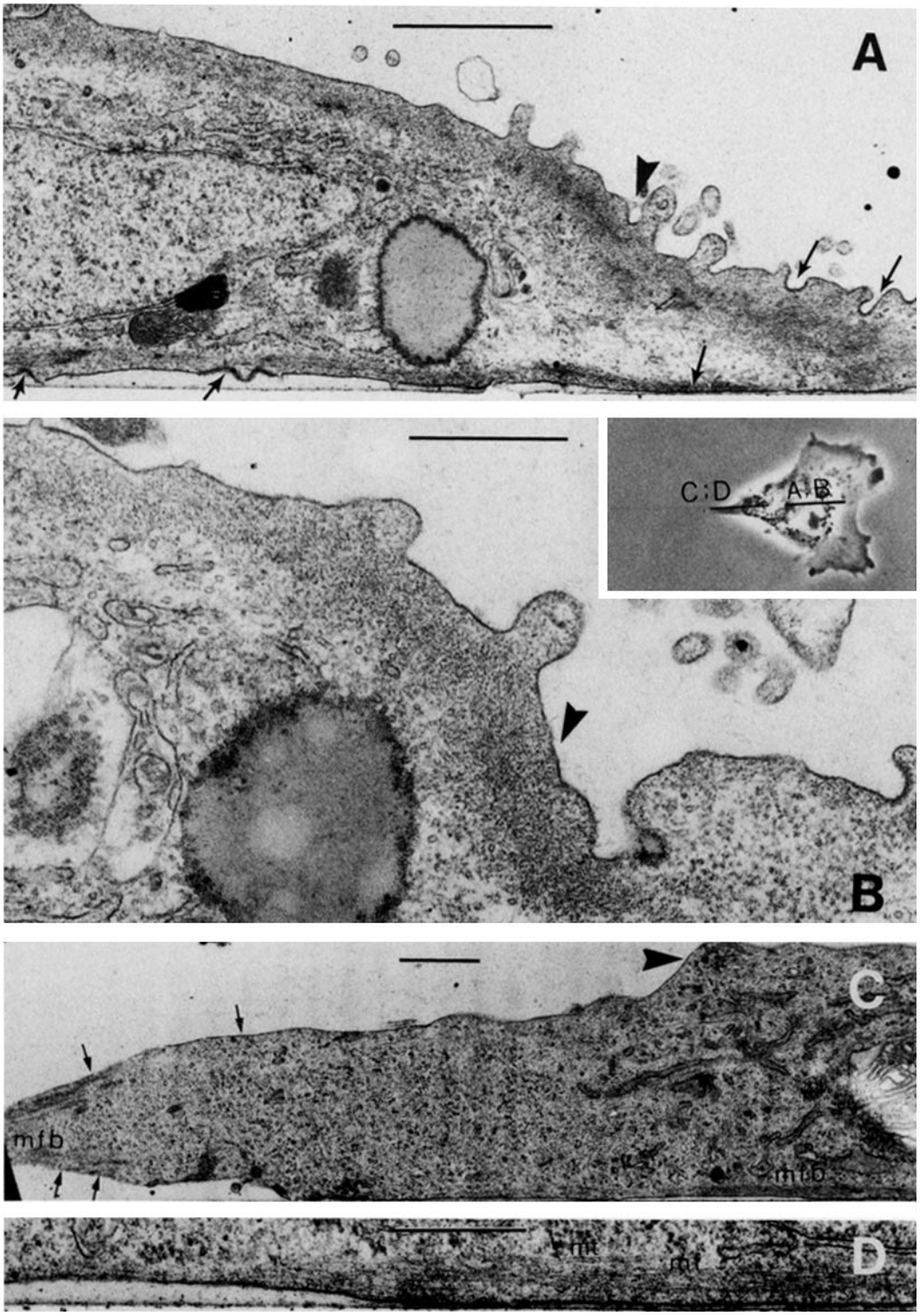

FIGURE 11 Ultrastructure of a fibroblast during the slow phase of retraction of the trailing edge. The phase-contrast image of the cell at the time of fixation, i.e., 46 s after detachment of the trailing edge, is inserted in *B*. The fixed cell is sectioned sagittally along the direction of tail retraction. Approximate positions of the TEM micrographs are indicated by lines in the fixed cell. (*A*) A section of the front of the cell body, around the region of null border (arrowhead; see also Fig. 4). The microfilament meshworks beneath the folded upper surface have an average thickness of 0.25 μm. Note the indentations and plaques, located in the cell surface of both upper and lower side of the cell (arrows), and the different orientation of cortical microfilaments in the upper and lower cytoplasm of the cell body. Cortical microfilaments between plaques are aligned in the form of "bundles". Bar, 1 μm. × 24,000. (*B*) A higher magnification of a section adjacent to the section shown in *A*. Arrowhead, the region of null border. Bar, 0.5 μm. × 48,000. (*C*) A sagittal section of the new tail (see the *insert* in *B*), posterior to the base of the retracted tail (arrowhead), showing its smooth surface and thin cortical layer. Bundles of microfilaments (*mgb*) extend beneath the smooth surface (arrows) in the new tail and at the lower side of the cell body in parallel with the direction of tension (see text). Bar, 1 μm. × 12,000. (*D*) A higher magnification of the lower side of the cell body showing smooth surface and oriented microfilaments (*mf*) and microtubules (*mt*). Bar, 0.5 μm. × 40,000.

by the meshwork in the slow phase completes retraction of the tail, throwing its surface into folds.

I am grateful to J. P. Trinkaus for advice during this research and for assistance in the preparation of this manuscript. I also wish to thank S. J. Singer for help in revising the manuscript, J. F. Ash, N. Orida, G. P. Radice, and M. S. Shure for helpful discussions, M. Trinkaus for editorial assistance, and Yun Yun Chen for aid with the illustrations.

This work represents part of a dissertation submitted to the Graduate School of Yale University in partial fulfillment of the requirements for the degree of Doctor of Philosophy and was supported by grants from the National Institutes of Health (HD 07137 and CA 22451) to J. P. Trinkaus and by Yale University Fellowships to W.-T.Chen.

Received for publication 17 September 1980, and in revised form 5 March 1981.

REFERENCES

1. Abercrombie, M., and G. A. Dunn. 1975. Adhesions of fibroblasts to substratum during contact inhibition observed by interference reflection microscopy. *Exp. Cell Res.* 92:57–62.
2. Abercrombie, M., G. A. Dunn, and J. P. Heath. 1977. The shape and movement of fibroblasts in culture. *In* Cell and Tissue Interactions. J. W. Lash and M. M. Burger, editors. Raven Press, New York. 57–70.
3. Abercrombie, M., J. E. M. Heaysman, and S. M. Pegrum. 1970. The locomotion of fibroblasts in culture. I. Movements of the leading edge. *Exp. Cell Res.* 59:393–398.
4. Abercrombie, M., J. E. M. Heaysman, and S. M. Pegrum. 1970b. The locomotion of fibroblasts in culture. III. Movements of particles on the dorsal surface of the leading lamella. *Exp. Cell Res.* 62:389–398.
5. Abercrombie, M., J. E. M. Heaysman, and S. M. Pegrum. 1971. The locomotion of fibroblasts in culture. IV. Electron microscopy of the leading lamella. *Exp. Cell Res.* 67: 359–367.
6. Algard, F. T. 1953. Morphology and migratory behavior of embryonic pigment cells studied by phase microscopy. *J. Exp. Zool.* 123:499–571.
7. Allen, R. D., D. W. Francis, and H. Nakajima. 1965. Cyclic birefringence changes in pseudopods of *Chaos carolinesis* revealing the localization of the motive force in pseudopod extension. *Proc. Natl. Acad. Sci. U. S. A.* 54:1153–1163.
8. Allen, R. D., and H. Nakajima. 1965. Two exposure, film densimetric measuring phase retardations due to weak birefringence in fibrillar or membranous cell constituents. *Exp. Cell Res.* 37:230–249.
9. Ambrose, E. 1961. The movement of fibrocytes. *Exp. Cell Res.* 8 (Suppl.):54–73.
10. Anderson, R. G. W., E. Vasile, R. J. Mello, M. S. Brown, and J. L. Goldstein. 1978. Immunocytochemical visualization fo coated pits and vesicles in human fibroblasts: relation to low density lipoprotein receptor distribution. *Cells* 15:919–933.
11. Balinsky, B. I. 1961. Ultrastructural mechanisms of gastrulation and neurulation. *In* Symposium on Germ Cells and Development. Institut Intern. d'Embryologie and Fondazione A. Baselli, Pavia. 550–563.
12. Begg, D. A., R. Rodewald, and L. I. Rebhun. 1978. The visualization of actin filament polarity in thin section. Evidence for the uniform polarity of membrane-associated filaments. *J. Cell Biol.* 79:846–852.
13. Betchaku, T., and J. P. Trinkaus. 1978. Contact relations, surface activity, and cortical microfilaments of marginal cells in the enveloping layer and of the yolk syncytial and yolk cytoplasmic layers of *Fundulus* before and during epiboly. *J. Exp. Zool.* 206:381–426.
14. Brunk, U., J. L. E. Ericsson, J. Ponten, and B. Westermark. 1971. Specialization of cell surfaces in contact-inhibited human glia-like cells *in vitro*. *Exp. Cell Res.* 67:407–415.
15. Buckley, I. K., and K. R. Porter. 1967. Cytoplasmic fibrils in living cultured cells. *Protoplasma.* 64:349–380.
16. Buckley, I. K., and T. R. Raju. 1976. Form and distribution of actin and myosin in non-muscle cells: a study using cultured chick embryo fibroblasts. *J. Microsc. (Oxf.).* 107:129–149.
17. Burnside, B. 1971. Microtubules and microfilaments in newt neurulation. *Dev. Biol.* 26: 416–441.
18. Carter, S. B. 1965. Principles of cell motility: the direction of cell movement and cancer invasion. *Nature (Lond.).* 208:1183–1187.
19. Carter, S. B. 1970. Cell movement and cell spreading: a passive or an active process? *Nature (Lond.).* 225:858–859.
20. Chen, W.-T. 1977. Retraction of the trailing edge during fibroblast movement. *J. Cell Biol.* 75 (2, Pt. 2): 411 *a* (Abstr.).
21. Chen, W.-T. 1979. Change in arrangement of cortical microfilaments associated with change in cell locomotor activity. *Biophys. J.* 25(2):32 *a* (Abstr.).
22. Chen, W.-T. 1979b. Induction of spreading during fibroblast movement. *J. Cell Biol.* 81: 684–691.
23. Chen, W.-T. 1981. Surface changes during retraction-induced spreading of fibroblasts. *J. Cell Sci.* In press.
24. Coman, D. R. 1944. Decreased mutual adhesiveness, a property of cells from squamous cell carcinomas. *Cancer Res.* 4:625–629.
25. Culp, L. A. 1976. Molecular composition and origin of substrate attached material from normal and virus-transformed cells. *J. Supramol. Struct.* 5:239–255.
26. Curtis, A. S. G. 1964. The mechanism of adhesion of cells to glass. A study by interference reflection microscopy. *J. Cell Biol.* 20:195–215.
27. Dunn, G. A. 1980. Mechanisms of fibroblast locomotion. *In* Cell Adhesion and Motility. A. S. G. Curtis and J. D. Pitts, editors. Cambridge University Press, Cambridge. 409–423.
28. Edidin, M., and A. Weiss. 1972. Antigen cap formation in cultured fibroblasts: a reflection of membrane fluidity and of cell motility. *Proc. Natl. Acad. Sci. U. S. A.* 69:2456–2459.
29. Erickson, C. A., and J. P. Trinkaus. 1976. Microvilli and blebs as sources of reserve surface membrane during cell spreading. *Exp. Cell Res.* 99:375–384.
30. Fay, F. S. 1976. Structural and functional features of isolated smooth muscle cells. *In* Cell Motility. Cold Spring Harbor Conference on Cell Proliferation, Vol. 1. R. Goldman, T. Pollard, and J. Rosenbaum editors. Cold Spring Harbor Laboratory, Cold Spring Harbor, N. Y. 185–201.
31. Fleischer, M., and K. E. Wohlfart-Botterman. 1975. Correlation between tension force generation, fibrillogenesis, and ultrastructure of cytoplasmic actomyosin during isometric and isotonic contraction of protoplasmic strands. *Cytobiologie* 10:339–365.
32. Follett, E. A. C., and R. D. Goldman. 1970. The occurrence of microvilli during spreading and growth of BHK21/C13 fibroblasts. *Exp. Cell Res.* 59:124–136.
33. Goldman, R. D., and D. M. Knipe. 1973. The functions of cytoplasmic fibers in non-muscle motility. *Cold Spring Harbor Symp. Quant. Biol.* 37:523–534.
34. Goldman, R. D., J. A. Schloss, and J. M. Starger. 1976. Organizational changes of actinlike microfilaments during animal cell movement. *In* Cell Motility. Cold Spring Harbor Conferences on Cell Proliferation, Vol. 3. R. Goldman, T. Pollard, and J. Rosenbaum, editors. Cold Spring Harbor Laboratory, Cold Spring Harbor, N. Y. 217–246.
35. Goodrich, H. B. 1924. Cell behavior in tissue cultures. *Biol. Bull. (Woods Hole).* 46:252–262.
36. Harris, A. 1973. Cell surface movements related to cell locomotion. *In* Locomotion of Tissue Cells, Ciba Foundation Symposium 14 (new series). Elsevier, North-Holland, Amsterdam. 3–26.
37. Harris, A. K. 1973. Behavior of cultured cells on substrate of variable adhesiveness. *Exp. Cell Res.* 77:285–297.
38. Harris, A. K. 1973. Location of cellular adhesions to solid substrata. *Dev. Biol.* 35:97–114.
39. Harris, A. K., P. Wild, and D. Stopak. 1980. Silicone rubber substrata: A new wrinkle in the study of cell locomotion. *Science (Wash. D. C.).* 208:177–179.
40. Harris, J. K. 1978. A photoelastic substrate technique for dynamic measurements of forces exerted by moving organisms. *J. Microsc. (Oxf.).* 114:219–228.
41. Heath, J. P., and G. A. Dunn. 1978. Cell to substratum contacts of chick fibroblasts and their relation to the microfilament system. A correlated interference-reflexion and high voltage electron-microscopy study. *J. Cell Sci.* 29:197–212.
42. Heaysman, J. E. M., and S. M. Pegrum. 1973. Early contact between fibroblasts. An ultrastructural study. *Exp. Cell Res.* 78:71–78.
43. Hoffmann-Berling, H. 1960. Other mechanisms producing movements. *In* Comparative Biochemistry. A Comprehensive Treatise. Vol. II. Free Energy and Biological Function. M. Florkin and H. S. Mason, editors. Academic Press, Inc., New York. 341–370.
44. Holtfreter, J. 1943. A study of the mechanics of gastrulation: part I. *J. Exp. Zool.* 94:261–318.
45. Isenberg, G., P. C. Rathke, N. Hulsmann, W. W. Franke, and K. E. Wohlfarth-Botterman. 1976. Cytoplasmic actomyosin fibrils in tissue culture cells-direct proof of contractility by visualization of ATP-induced contraction in fibrils isolated by laser microbeam dissection. *Cell Tissues Res.* 166:427–443.
46. Ishikawa, H., R. Bischoff, and H. Holtzer. 1969. Formation of arrowhead complexes with heavy meromyosin in a variety of cell types. *J. Cell Biol.* 43:312–328.
47. Izzard, C. S., and S. L. Izzard. 1975. Calcium regulation of the contractile state of isolated mammalian fibroblast cytoplasm. *J. Cell Sci.* 18:241–256.
48. Izzard, C. S., and L. R. Lochner. 1976. Cell-to-substrate contacts in living fibroblasts: An interference reflection study with an evaluation of the technique. *J. Cell Sci.* 21:129–159.
49. James, D. W., and J. F. Taylor. 1969. The stress developed by sheets of chick fibroblasts *in vitro*. *Exp. Cell Res.* 54:107–110.
50. Karfunkel, P. 1971. The role of microtubules and microfilaments in neurulation in *Xenopus*. *Dev. Biol.* 25:30–56.
51. Lewis, W. H., and M. R. Lewis. 1924. Behavior of cells in tissue cultures. *In* General Cytology. E. V. Chowdry, editor. The University of Chicago Press, Chicago. 385–447.
52. Lloyd, C. W., C. G. Smith, A. Woods, and D. A. Rees. 1977. Mechanisms of cellular adhesion. II. The interplay between adhesion, the cytoskeleton, and morphology in substrate-attached cells. *Exp. Cell Res.* 110:427–437.
53. Luduena, M. A., and N. K. Wessells. 1973. Cell locomotion, nerve elongation, and microfilaments. *Dev. Biol.* 30:427–440.
54. Maroudas, N. G. 1973. Chemical and mechanical requirements for fibroblast adhesion. *Nature (Lond.).* 244:353–354.
55. Nagai, R., Y. Hoshimoto, and N. Kamiya. 1978. Cyclic production of tension force in the plasmodial strand of *Physarum polycephalum* and its relation to microfilament morphology. *J. Cell Sci.* 33:205–225.
56. Porter, K. R. 1978. Organization in the structure of the cytoplasmic ground substratum. Ninth International Congress on Electron Microscopy. 3:627–639.
57. Schroeder, T. E. 1973. Cell constriction: contractile role of microfilaments in division and development. *Am. Zool.* 13:949–960.
58. Singer, S. J., and G. L. Nicolson. 1972. The fluid mosaic model of the structure of cell membranes. *Science (Wash. D. C.).* 175:720–731.
59. Spooner, B. S., J. F. Ash, J. T. Wrenn, R. B. Frater, and N. K. Wessells. 1973. Heavy meromyosin binding to microfilaments involved in cell and morphogenetic movements. *Tissue Cell.* 5:37–46.
60. Spooner, B. S., K. M. Yamada, and N. K. Wessells. 1971. Microfilaments and cell locomotion. *J. Cell Biol.* 49:595–613.
61. Taylor, D. L., J. S. Condeelis, P. L. Moore, and R. D. Allen. 1973. The contractile basis of amoeboid movement. I. The chemical control of motility in isolated cytoplasm. *J. Cell Biol.* 59:378–394.
62. Trinkaus, J. P. 1951. A study of the mechanism of epiboly in the egg of *Fundulus heteroclitus*. *J. Exp. Zool.* 118:269–319.
63. Trinkaus, J. P. 1976. On the mechanism of metazoan cell movements. *In* The Cell Surface in Animal Embryogenesis and Development. G. Poste and G. L. Nicolson, editors. *Cell Surf. Rev.* 1:225–329.
64. Trinkaus, J. P., T. Betchaku, and L. S. Krulikowski. 1971. Local inhibition of ruffling during contact inhibition of cell movement. *Exp. Cell Res.* 64:291–300.
65. Weiss, L. 1961. The measurement of cell adhesion. *Exp. Cell Res.* 8 (Suppl.):141–153.
66. Weiss, L. 1976. Biophysical aspects of the metastatic cascade. *In* Fundamental Aspects of Metastasis. L. Weiss, editor. North-Holland Publishing Co., Amsterdam. 51–70.
67. Weiss, L., and R. R. A. Coombs. 1963. The demonstration of rupture of cell surfaces by an immunological technique. *Exp. Cell Res.* 30:331–338.
68. Weiss, P., and B. Garber. 1952. Shape and movement of mesenchyme cells as functions of the physical structure of the medium. Contributions to a quantitative morphology. *Proc. Natl. Acad. Sci. U. S. A.* 38:264–280.